THE PENNSYLVANIA STATE UNIVERSITY
SCHREYER HONORS COLLEGE

DEPARTMENT OF CHEMICAL ENGINEERING

Lithium Salt Doping of Organic Photovoltaics

BRYAN P. WILLIAMS
FALL 2013

A thesis
submitted in partial fulfillment
of the requirements
for a baccalaureate degree
in Chemical Engineering
with honors in Chemical Engineering

Reviewed and approved* by the following:

Enrique D. Gomez
Assistant Professor of Chemical Engineering
Thesis Supervisor

Wayne Curtis
Professor of Chemical Engineering
Honors Adviser

* Signatures are on file in the Schreyer Honors College.

ABSTRACT

Charge recombination and low charge mobility significantly hinders the performance of organic solar cells with thin active layers. In an effort to overcome these obstacles, lithium salt was added to a novel polymer, M-TQ1, blended with an electron acceptor, PCBM, in an attempt to increase dielectric permittivity and hole mobility, in order to improve organic photovoltaic (OPV) performance. This hypothesis was tested with organic field-effect transistors (TFT), TEM imaging, and performance of fabricated polymer solar cells. Lithium salt-doping was found to be an effective additive to increase both hole mobility and charge recombination lifetime. These experiments demonstrated increases of two orders of magnitude in hole mobility and almost an order of magnitude in recombination lifetime in the lithium-doped M-TQ1. However, these improvements did not translate seamlessly to enhancements in solar cell performance. Inadequacies in the morphology, namely phase separation, of PCBM/M-TQ1 solar cells prevented the majority of the excitons from reaching the blend interface, proving to be detrimental to device performance. If issues associated with the active layer morphology could be resolved, the improvements to electronic properties with lithium salt doping seen in TFT measurements could one day be translated to polymer solar cells, which could prove to be a revolutionary advance in our energy infrastructure.

TABLE OF CONTENTS

LIST OF FIGURES

ACKNOWLEDGEMENTS

I would like to thank the National Science Foundation for financial support on this project under Award DMR-1056199. I'd also like to thank my research advisor, Dr. Enrique D. Gomez, for his guidance and support throughout my three years working in his lab. Kiarash Vakhshouri and Changhe Guo helped significantly with data and imaging acquisition, so I'd like to thank them as well. Also, thank you to the Asbury Group in the Department of Chemistry and Wang Group in the Materials Science and Engineering Department for their significant contributions to my project. Being a member of the Schreyer program has opened many doors for me during my time here at Penn State, so I'd like to acknowledge their funding and guidance during my time at this university. Finally, I'd like to thank my parents, Don and Janine Williams, for providing me every opportunity that I have had, and for plenty of guidance along the journey.

Chapter 1

Introduction

The ability to produce technology to efficiently harness and utilize the sun's light has been an ambition of humankind for millennia. As early as the 3rd century BC, Romans and Greeks concentrated sunlight using magnifying pieces of glass and mirrors to ignite fires for warmth and religious ceremonies. In the centuries that followed, solar energy became a versatile tool across many cultures for the purposes of heating specially-designed buildings, water heating, cooking, and powering steam engines.[1] The value of the sun's energy as a source of electricity was not realized until 1839, when French physicist Edmond Becquerel discovered the photovoltaic effect upon observing improved illumination in an ionic solution with submerged electrodes when exposed to sunlight.[2] However, the breakthrough in physics that most influenced the photovoltaic technology commonly seen in our infrastructure today was the discovery of the photoconductivity of selenium by English electrical engineer Willoughby Smith in 1873.[1]

The first generation of photovoltaic technology was conceived by a group of American scientists at Bell Labs in 1954 using crystalline silicon. The first generation of solar cells is characterized by the use of semiconducting p-n junctions created by small amounts of dopant in the silicon. The original solar cells were only 6% efficient in converting the sun's energy to electricity; nonetheless, silicon based solar cells have been developed into the prominent devices in the industry today.[1] The dominance of a silicon photoactive layers stems from its relative natural abundance and current efficiencies in production modules of up to 20%. However, the manufacturing of these devices is an arduous and costly process, requiring the growth of silicon crystals at a purity of 99.999%. This purity provides optimum mobility to free electrons generated

by sunlight. The inflexibility and limited lifetimes of the devices have necessitated improved photoactive materials if solar is to compete with other energy technologies.[3]

The goal of second generation solar technologies has emerged to reduce the manufacturing costs of solar cells by utilizing thin film design. Using less photoactive material and resulting in a less brittle device, thin film solar modules have a limited efficiency of 9% in the field, but further research is projected to drive thin film efficiency to compete with crystalline silicon technology.[4] Although thin films are a marked improvement, manufacturing challenges and limited resources still leave the door open for emerging third generation solar technologies. This generation encompasses a wide array of possible photoactive layers that share the characteristic of the ability to transcend the Shockley-Queisser theoretical limit of 41% power efficiency. However, the majority of these technologies have limited stabilities and tested efficiencies which have thus far prevented their industrial production.[5] Figure 1.1 details the advance of world-record efficiencies for photoactive layer materials from all of the areas of photovoltaic research, including multijunction, single-junction gallium arsenide, crystalline silicon, thin films, and other emerging PV technology.[6]

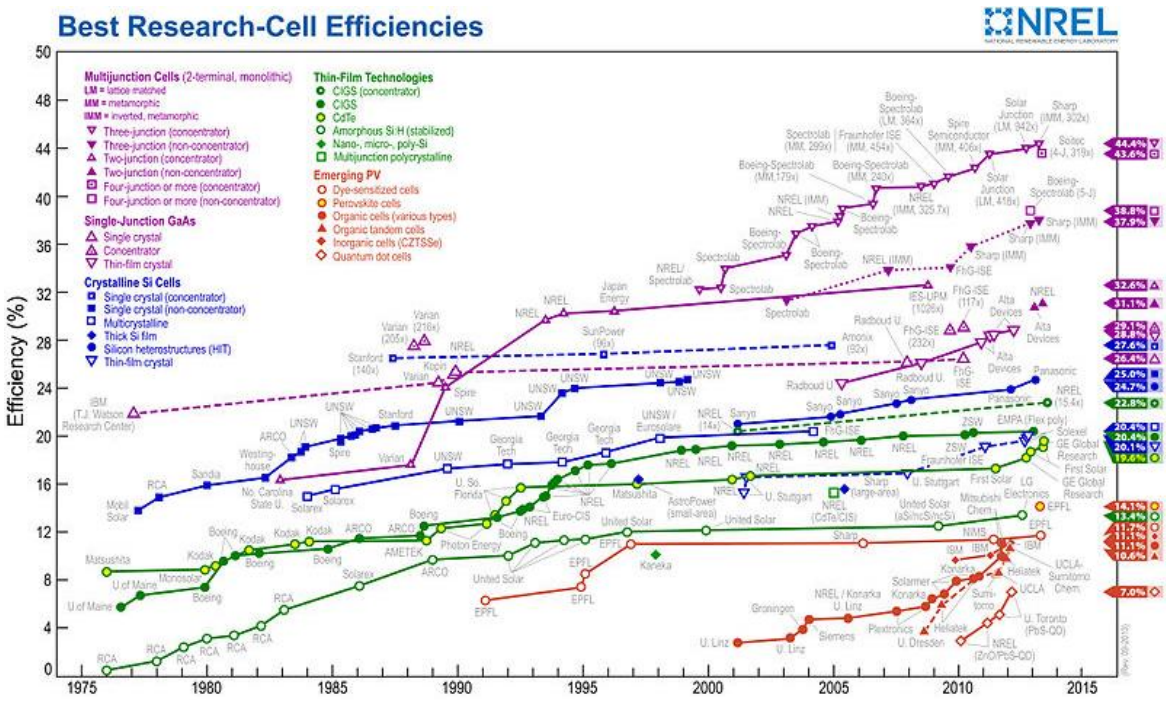

Figure 1-1. Progression of Record Solar Cell Efficiency for Each Type of Technology[6]

Chapter 2

Theory

Thin film solar cell technology includes a branch of organic photovoltaics (OPV) which utilize the semiconducting properties of certain conjugated polymers. Bulk heterojunction photovoltaics are a type of organic device composed of a blend of a semiconducting polymer donor and a fullerene-based electron acceptor that we commonly fabricated in the Gomez lab. When sunlight hits these materials, excitons, which are electron-hole pairs, are generated. In Figure 2.1, the cross-sectional structure of this type of photovoltaic device is shown.

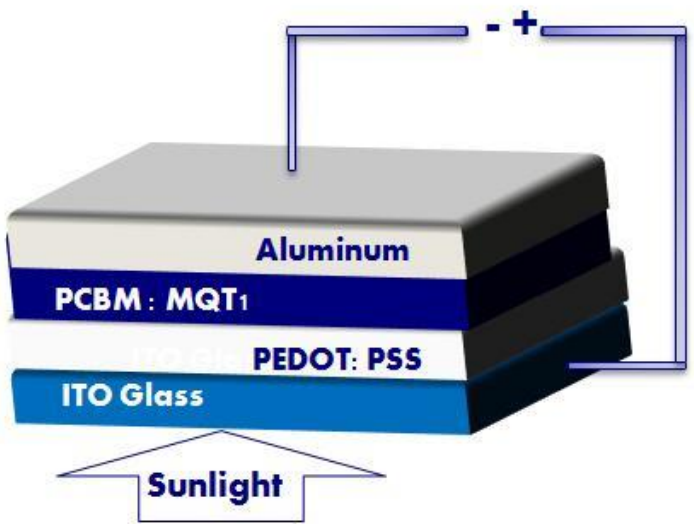

Figure 2-1. Schematic of a Bulk Heterojunction Photovoltaic Device

At the interfaces that form between the two materials in the active layer, the excitons can split, causing the electrons to move to the electron acceptor domains and subsequently the aluminum electrodes. The holes travel to the other side of the photoactive layer to the indium tin oxide (ITO) electrode, and both charges flow outside of the cell to perform work and return to the

photoactive layer on the opposite side from which they left.[7] An electron-blocking layer of PEDOT:PSS is commonly utilized on the ITO glass electrode side of the photoactive layer to prevent electrons from flowing opposite to the intended direction. The most commonly studied polymer-fullerene blend in the past has been poly(3-hexylthiophene) (P3HT) and phenyl-C_{61}-butyric acid methyl ester (PCBM), and conversion efficiencies of over 5% have been achieved with this photoactive layer formula.

In polymer organic photovoltaic (OPV) materials, geminate and bimolecular charge recombination have deleterious effects on performance.[8] Researchers attempt to minimize the negative effects of these processes by limiting the thickness of organic photovoltaic active layers to about 100 nm.[9-12] In photoactive layers this thin, highly efficient charge collection is enabled because charge carrier travel time within the device is less than the average time it takes for recombination of charges.[13] However, at this thickness the active layers are too thin to capture all of the light that hits the device, particularly at long wavelengths. The relatively high performance of P3HT: PCBM devices can be attributed to long recombination lifetimes coupled with high charge carrier mobility, but the reason for this unique property is not well understood. The goal of this research field is to reproduce these properties in a wide range of organic semiconductors to continue to further develop high efficiency organic solar cells.

It would be advantageous to increase the mobility-lifetime of organic semiconductors to enable longer charge diffusion lengths, thus enabling thicker active layers to capture more incident photons. The addition of salts to organic semiconductors to improve electronic performance was recently studied in solid state dye sensitized solar cells.[14, 15] In that study, the presence of LiTFSI enhanced not only the charge carrier mobility but also the charge recombination lifetime when added to the solid state hole conductor of the device. The lengthened charge recombination lifetime was explained by the screening of electrons and holes by the presence of lithium ions near photovoltaic electrode interfaces.[14, 16] This work found there

was a decrease in energetic barrier to charge transport because a reduction in screening length effectively lowered the Coulomb trapping energies of holes. My project was conducted based on the hypothesis that the beneficial effects of the addition of LiTFSI to solid state dye-sensitized solar cells may be applicable to organic solar cells. It was believed that the improved performance would result from influencing the dielectric permittivity and doping of the photoactive layer materials. My contribution to the study was a fundamental study of the charge carrier dynamics and photovoltaic device performance in an ion-doped polymer blend photovoltaic material.

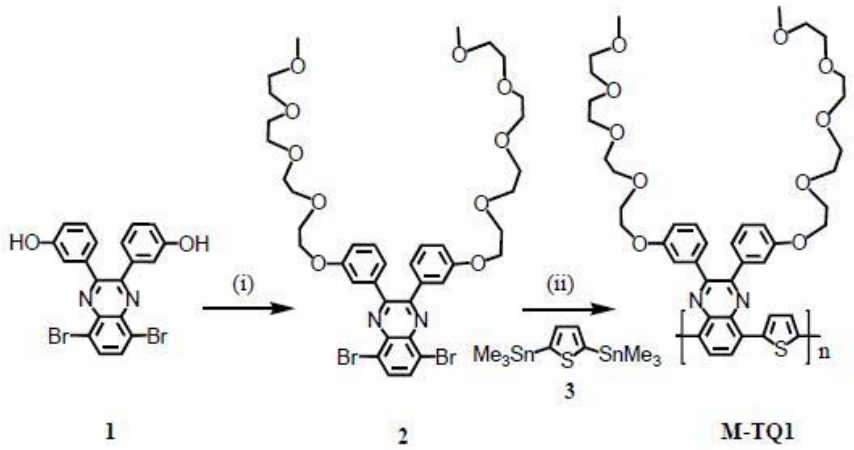

Figure 2-2. Reaction Mechanism for the Synthesis of M-TQ1

For this project, my research group combined electrical characterization, time-resolved infrared spectroscopy and electron microscopy to explore if the electronic performance of a conjugated polymer called M-TQ1, which was specially synthesized to coordinate lithium ions, can be enhanced by the addition of LiTFSI. The reaction mechanism for this novel polymer is shown above in Figure 2-2.[17]

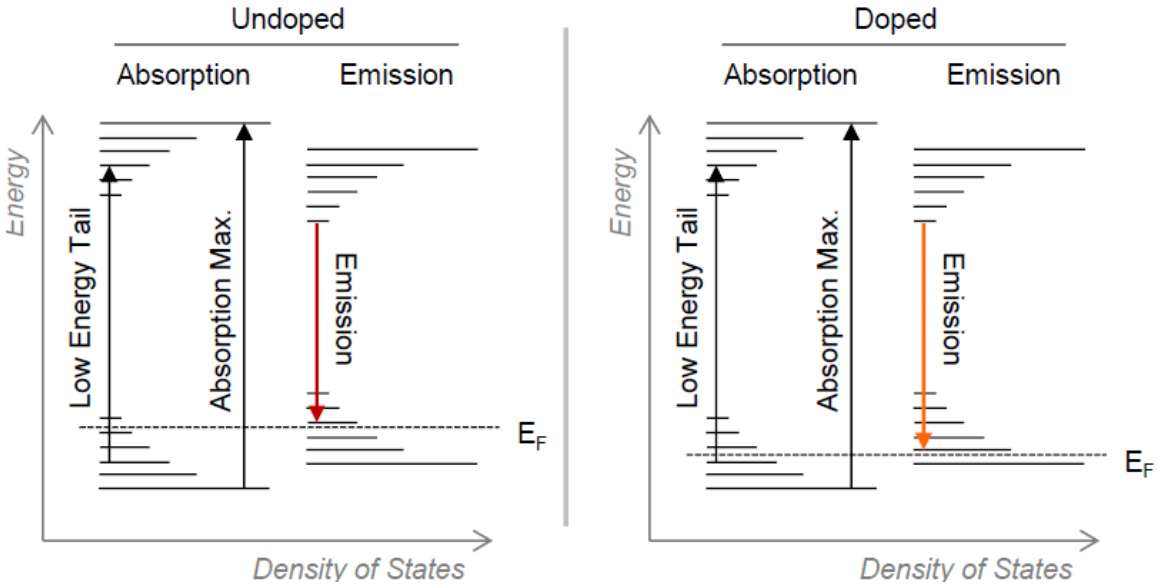

Figure 2-3. Physics of Photoluminescence with Li Salt Doping

The current explanation of the positive effects that lithium salt doping may have on an organic semiconductor can be explained with Figure 2-3.[17] After a photon of light is absorbed, the exciton transitions toward the lowest possible energy state above the effective Fermi energy (E_F). The lithium salt affects this process by lowering the effective Fermi energy, which causes greater hole density at the valence level, resulting in greater hole mobility. This phenomenon results in a higher energy emission which could yield an increase in photovoltaic or transistor performance.

Chapter 3

Experimental Procedure of Photovoltaic Fabrication

To prepare salt solutions, residual water was removed from the LiTFSI by heating for two days at 150 ^{o}C in a glovebox antechamber. To prevent exposure to ambient atmosphere, LiTFSI was moved directly into a N_2 glovebox and dissolved in anhydrous tetrahydrofuran (Sigma-Aldrich) for 12 hours at 5 wt % concentration. Solutions of M-TQ1 and PCBM (>99.5%, Nano-C), 1:3 by mass, were made with anhydrous 1,2-dichlorobenzene (Sigma-Aldrich). LiTFSI salt was added by pipetting the corresponding volume of the LiTFSI/THF solution to yield the proper Li^{+}/O ratio desired. Vials containing M-TQ1, PCBM, and LiTFSI solutions were stirred for 1 hour minimum at 100 °C before spin coating to ensure proper dissolution. These same solutions were used to cast films for the TFT, photovoltaic, and TRIR measurements. Solar cells with a device area of 0.162 cm^2 were fabricated on indium tin oxide (ITO) coated glass substrates (Kintec, Hong Kong). The substrates were cleaned with Aquet detergent solution and water, followed by 10 minutes of sonication in acetone, 10 minutes in isopropanol, and 10 minutes of UV-ozone treatment. PEDOT:PSS was spun cast hood at 4000 rpm for 2 minutes within a laminar flow and subsequently dried at 165 °C for 10 minutes to achieve a thickness of 70 nm. M-TQ1/PCBM with an active layer solution concentration of 24 mg/mL were subsequently spun cast in a N_2 glovebox at 1000 rpm for 1 minute on top of the PEDOT:PSS layer for a thickness of 65 ± 10 nm. Finally, a 75 nm layer of aluminum was deposited on top of the active layer via thermal evaporation at a pressure of 10^{-6} torr. All devices were annealed at 100 ^{o}C for 20 minutes. The electrical characterization of photovoltaic devices in the dark and under AM 1.5G (100 mW/cm^2) illumination from a 150 W Newport solar simulator was performed using a Keithley 2636A Sourcemeter. All data was averaged over at least 6 identical devices, and the fabrication and testing was conducted in a N_2 glovebox while avoiding sample exposure to ambient

atmosphere.[17] Figure 3-1 shows the fully fabricated organic photovoltaic device used in the tests for this study.

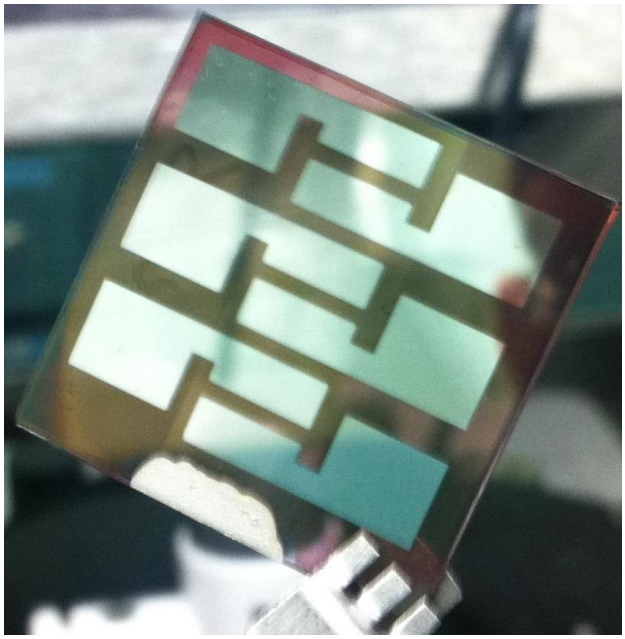

Figure 3-1. Fabricated Polymer Photovoltaic Device

Chapter 4

Results

The distribution of lithium ions uniformly throughout the organic phase was essential to tune the dielectric properties of polymer semiconductors in this study. This goal is particularly important because individual ions or small groups of them have the ability to respond readily to local fluctuations in electrostatic potential. In order to properly separate the lithium cations, a low band-gap conjugated polymer with ethylene oxide side chains was synthesized according to the mechanism in Figure 2-2. Initially, there was some concern that the salt would cause oxidation or reduction chemistry on the polymer, but the potentials of LiTFSI are outside of the corresponding potentials of the conjugated polymer.[18,19] This same salt was previously used to dope hole transport layers in solid state dye-sensitized solar cells, which was the inspiration for this project.[20]

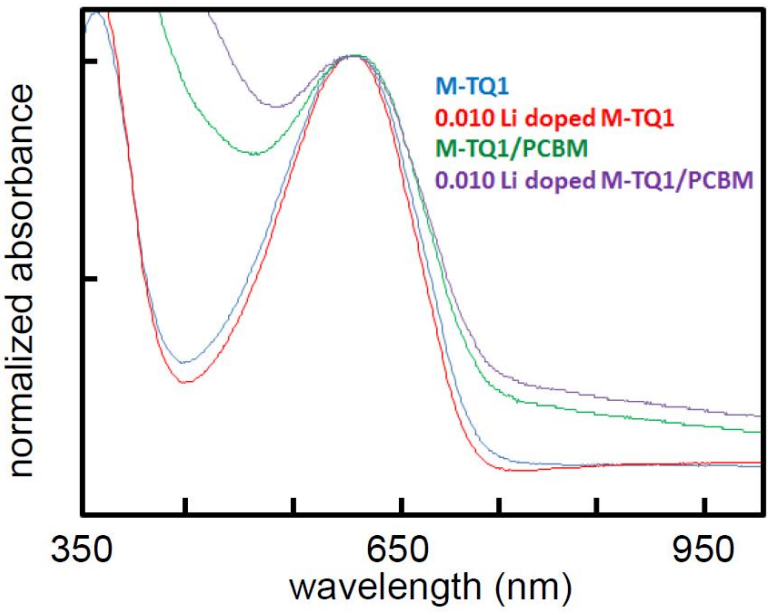

Figure 4-1. Normalized Visible Absorption and Emission Spectra of M-TQ1 Films

In Figure 4.1, an optical bandgap of M-TQ1 of 1.7 eV with an absorption maximum at 620 nm was found in the superimposed emission and absorption spectra. The films of Li-doped M-TQ1 (Li+/O = 0.010) and pure M-TQ1 have emission spectra that are nearly identical. The addition of lithium salt is shown to have little effect on the spectrum of the 1:1 by mass blend of M-TQ1 with PCBM. These findings signify that the coordination of lithium ions to ethylene oxide side chains of the polymer do not change the conjugated framework, which is essential to the material's function as a semiconductor in the photoactive layer.

Bottom-contact, bottom-gate field-effect-transistors (TFT) were utilized to characterize the influence of ion-doping on the hole mobility in M-TQ1. The TFT geometry is represented below in Figure 4-2.

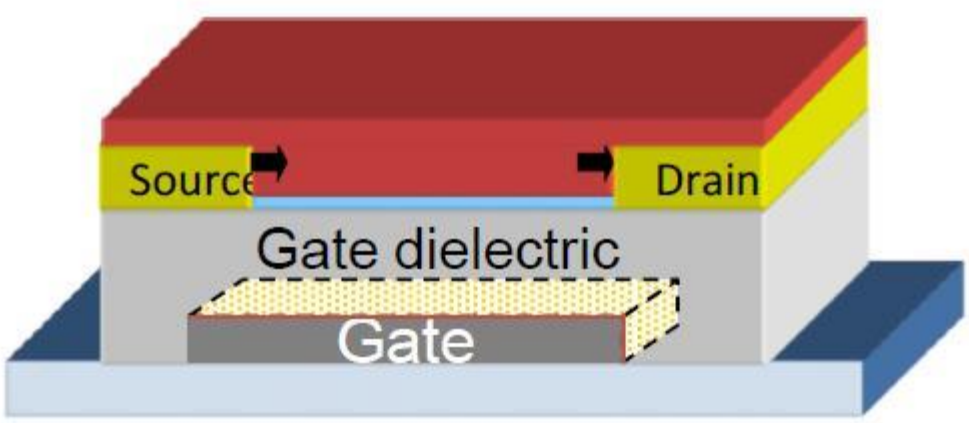

Figure 4-2. Diagram of a Field-Effect Transistor for Measuring Hole Mobility

Heavily doped p-type Si wafers were used as the gate electrodes with a 300 nm-thick thermally grown SiO_2 layer as the gate dielectric. Gold source and drain electrodes (with the thickness of ~ 100 nm) were deposited by conventional double-layer lithography with channel widths of 220 μm and lengths of 20 μm. Device testing was performed in a N_2 glovebox.[17] The source-drain current, I_{SD}, versus gate voltage, V_g, characteristics of TFTs prepared with LiTFSI concentrations are shown in Figure 4-3.

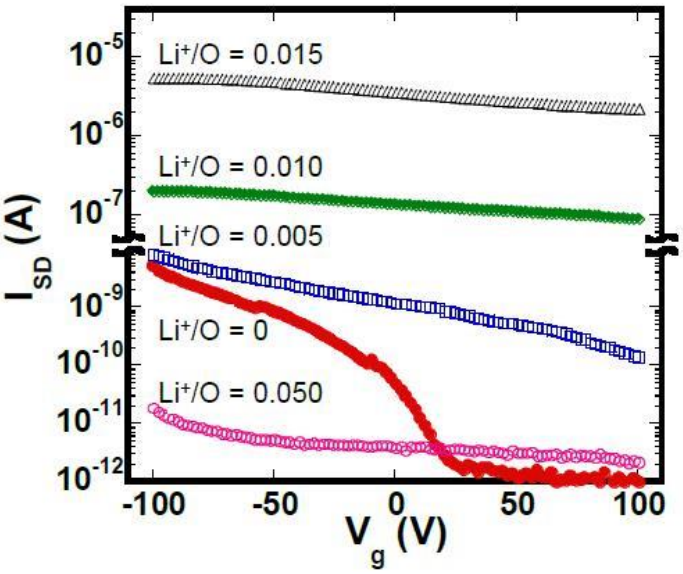

Figure 4-3. Source Drain Current vs. Gate Voltage for Different M-TQ1 Films

These salt concentrations correspond to 0, 0.05, 0.1, 0.15, and 0.5 lithium ions for each monomer in the polymer. The addition of lithium salt increased the I_{SD} for both negative (on) and positive (off) V_g values. The differential mobilities of the TFTs at saturation (V_{SD} = –50 V) calculated and shown in Figure 4-4 reveal a two orders of magnitude increase the hole mobility with increasing Li^+/O ratio up to a value of 0.015.

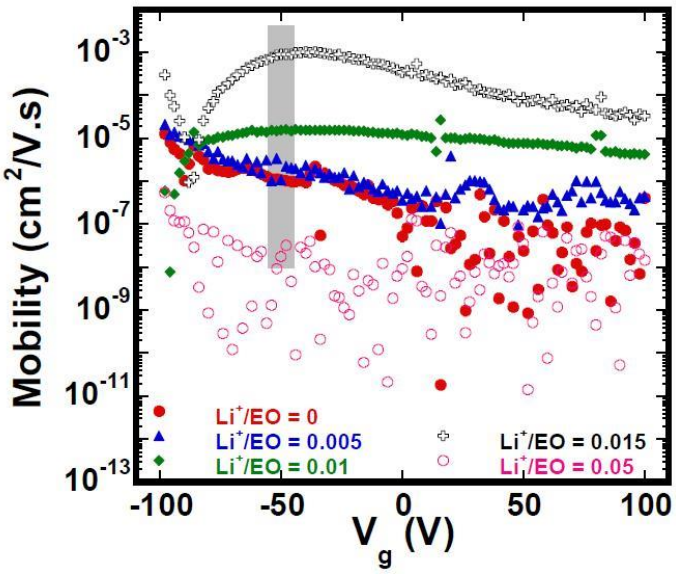

Figure 4-4. Differential Mobilities for M-TQ1 TFT Films

The I_{SD} level decreases significantly (to the order of 10^{-11} A) at the Li+/O ratio of 0.05 resulting in a hole mobility that decreases one or two orders of magnitude compared to pure M-TQ1. Figure 4-5 shows a summary of 1:3 M-TQ1: PCBM photovoltaic device characteristics as a function of salt concentration in the active layer.

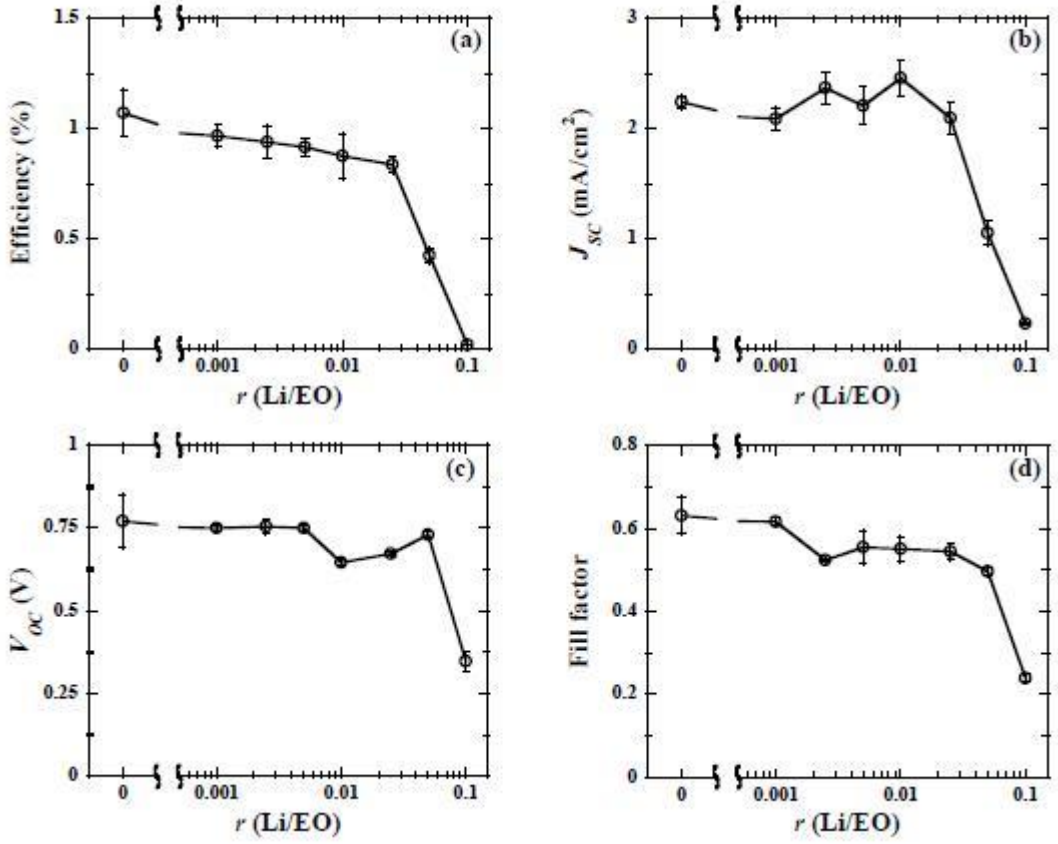

Figure 4-5. Photovoltaic Device Performance Parameters ((a) efficiency, (b) short-circuit current, (c) open circuit voltage, (d) fill factor) at Each Li/EO Concentration¥

The important parameters shown are the conversion efficiency, the short circuit current (value of J when voltage is zero), the open circuit voltage (value of V when the current is zero), and the fill factor of the device, respectively. The current (J) and voltage (V) curves for photovoltaic devices in Figure 4-6 show the characteristic performance of the solar cells under illumination (first two plots) and in the dark (last plot). Figure 4-6a shows a sharp increase in the current near -1 V, which typically indicates open leakage pathways that have a deleterious effect on device

performance. As the salt concentration is increased, the doping of M-TQ1 by the lithium salt results in higher reverse saturation currents as seen in Figure 4-6c, leading to a drop in the open circuit voltage. This plot also shows that in the dark, current is substantially lower in devices with high salt concentration, suggesting that hole mobility is responsible for poor device performance.

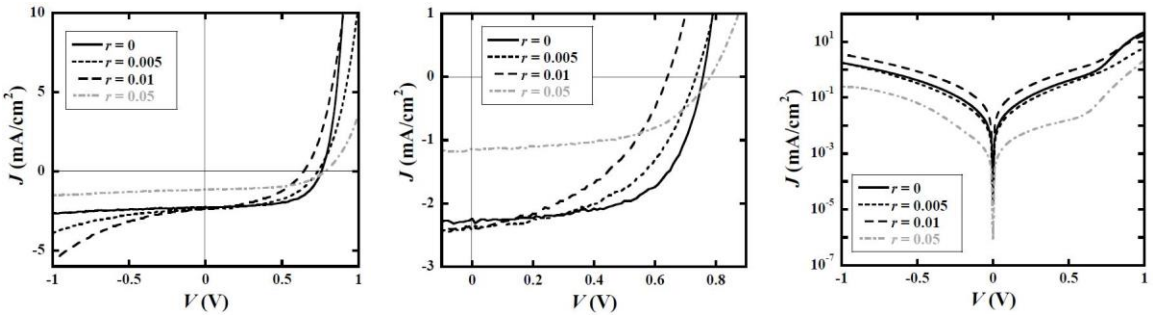

Figure 4-6.Current-Voltage (JV) Plot for Photovoltaic Devices at Each Li/EO wt. Ratio (r)

Figure 4-7 shows a carbon map from an energy filtered TEM images of a 1:3 (by mass) M-TQ1:PCBM polymer blend after having been annealed at 100 ^{o}C for 10 minutes.

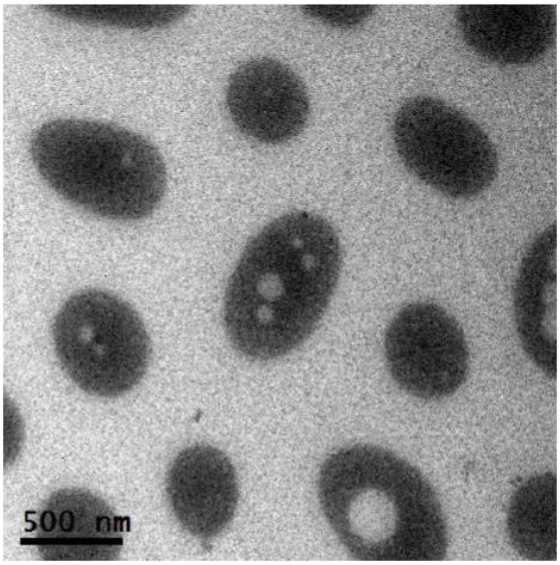

Figure 4-7. Energy Filtered TEM Image of 1:3 by Mass M-TQ1/PCBM[¥]

This film used for the TEM measurements has no LiTFSI added. These films of mass ratio 1:3 M-TQ1: PCBM give insight into factor that affects the power conversion efficiency measurements above. The M-TQ1 and PCBM undergo macroscopic phase separation, shown in the carbon map

by the oval shaped objects, which consist mostly of M-TQ1, that are imbedded in the lightly-shaded PCBM-rich phase. The thermal annealing of the film, which is also the final step before testing the photovoltaic devices, should not affect the polymer blend morphology.

Chapter 5

Discussion & Conclusions

The results of this research help to clarify the influence that lithium ion-doping has on the electronic properties of the M-TQ1/PCBM polymer blends.

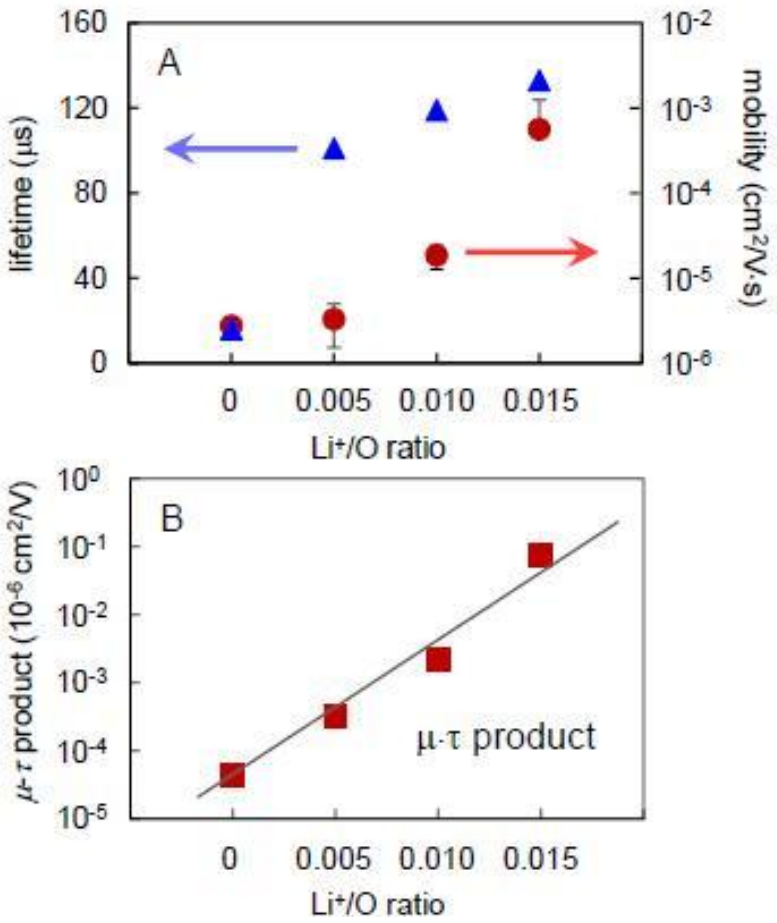

Figure 5-1.(A) Plot of Increase in Hole Mobility and Charge Recombination Lifetime (B) Mobility-Lifetime Product at Various Salt Concentrations[¥]

Figure 5-1A compiles the TFT data showing variation of the hole mobility (right axis) and bimolecular charge recombination lifetime (left axis) at all lithium salt concentrations. Figure 5-1B displays the product of these two parameters, mobility-lifetime, which increases continuously,

which gives evidence for the enhancement of the dielectric constant of the doped polymer. The mobility increased from 10^{-6} cm^2/Vs to 10^{-3} cm^2/Vs with an increasing Li^+/O ratio up to 0.015. However, for the TFT with a Li^+/O ratio of 0.050, the hole mobility decreased to less than 10^{-7} cm^2/Vs (from Figure 4-4). A possible explanation for this drop could be accumulation of the lithium salt at the semiconductor gate dielectric interface at these higher salt concentrations. The presence of this abundance of salt could disrupt the measurement since conduction happens very close to this dielectric interface. Another explanation is that strong columbic interactions at high salt concentrations may actually hinder the movement of charges within the active layer, reducing mobility. The source-drain current at positive gate voltages increases significantly with ion-doping as seen in Figure 4-3. Without lithium ions, the off-current is of the order 10^{-12} A, which is the minimum detection limit of this instrument. But when lithium ions are added at Li+/O = 0.015, the off-current increases six orders of magnitude to 10^{-6} A for the same device area. Because conductivity is the product of carrier mobility and density, this increase steams from a combination of an increase in both the density of holes and in their mobility in the film. Given that the mobility increased by two orders of magnitude, we conclude that the density of holes increased markedly with the incorporation of lithium ions into the film. The reason behind the increase in hole mobility is the filling of deep trap states such that conduction of holes occurs through states that are nearer to the hole mobility edge.

The energy filtered TEM image in Figure 5 explains the small reduction of photoluminescence lifetime when PCBM is introduced in photovoltaic devices. From this image, an approximately 500 nm scale phase separation is observed, which suggests that only about 10% of the total M-TQ1 is within the 10 nm exciton diffusion length of the PCBM-rich phase. Therefore, 90% of the M-TQ1 in the polymer blend is not affected by the addition of this electron acceptor. This conclusion is based on the assumption of a spherical model of M-TQ1 clusters and ignores that small amounts of M-TQ1 could exist in the PCBM-rich phase, or PCBM in the M-

TQ1 clusters. If 90% of the semiconducting polymer is not within 10 nm of PCBM-rich phase, then significantly less excitons will be split. Therefore, the resultant coarse phase separation of the PCBM/M-TQ1 active layer is not conducive to exciton splitting and high performance in organic solar cells.

Despite this morphological inadequacy, the devices without salt doping are still able to achieve 1% power conversion efficiency. This efficiency, shown in Figure 4-5, decreases slowly with addition of salt until the Li+/O ratio reaches 0.03, after which the performance drops off even more rapidly. This sudden decrease in performance is due to the strongly suppressed hole mobility in M-TQ1 at higher salt concentrations mentioned earlier. The other photovoltaic parameters measured, including the short-circuit current (J_{SC}), open-circuit voltage (V_{OC}), and fill factor stay relatively constant at low salt concentrations. The decrease in V_{OC} at a Li+/O ratio of 0.01 could be caused by an increase in leakage pathways because of increasing numbers of free charge carriers. Another explanation for this drop is that salt ions could be migrating in the applied electric field resulting in a salt concentration gradient. There is a brief increase of the V_{OC} at a Li+/O ratio of 0.05 which could be due to suppressed hole mobility in M-TQ1, which creates a space-charge region in the photovoltaic device. The increase in the V_{OC} at a Li+/O ratio is 0.05 is related to a drop in the J_{SC}. Unfortunately, no significant enhancement in any of the photovoltaic performance metrics is apparent in M-TQ1: PCBM OPVs despite the marked increase in mobility-lifetime product with salt addition. The lack of device performance with lithium salt is likely due to the coarse phase separation and doping effect that the salt has on the conjugated M-TQ1. This coarse phase separation is caused by the ethylene oxide side chains in M-TQ1, which makes the conjugated polymer more polar and hydrophilic, which reduces its compatibility with PCBM in organic photovoltaic devices.

Appendix A

Supplementary Project Data

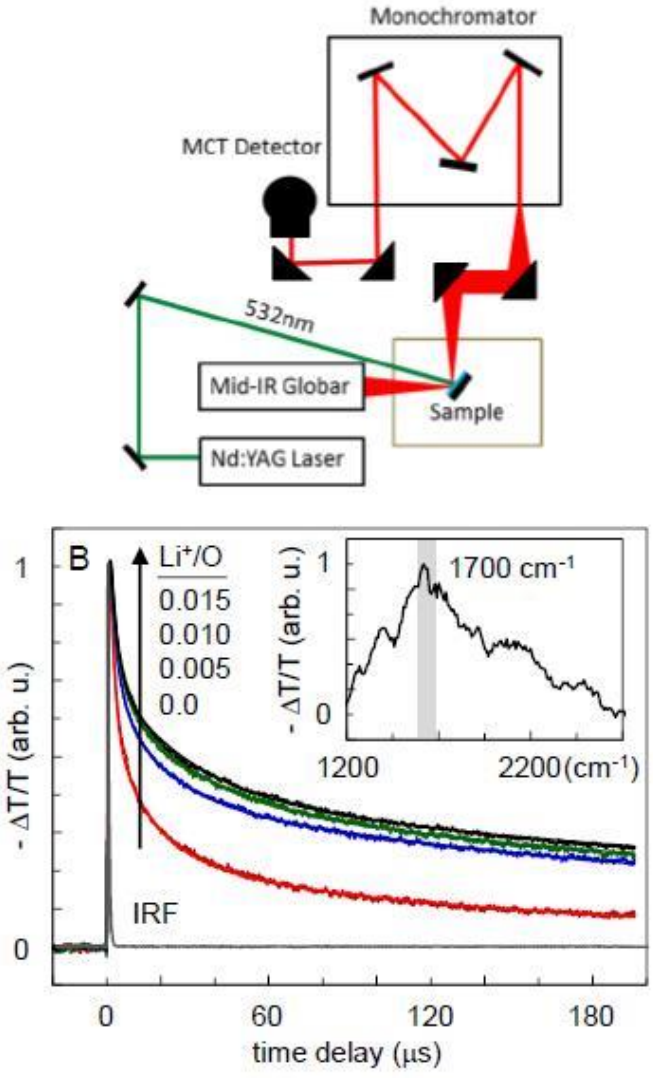

Figure 5-2. Design of the TRIR Instrument Used to Measure Charge Recombination Kinetics and Charge Recombination Kinetics for Various Concentrations of Lithium Ions[¥]

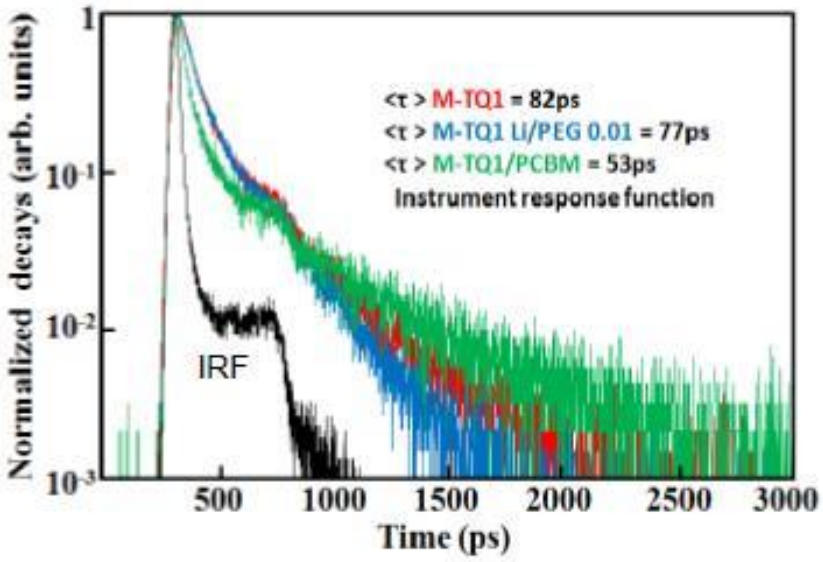

Figure 5-3. Excitation Lifetime of M-TQ1 at Various Salt Concentrations

BIBLIOGRAPHY

1. "The History of Solar." Energy Efficiency and Renewable Energy. US Department of Energy, n.d. Web. 1 Nov. 2013. <http://www1.eere.energy.gov/solar/pdfs/solar_timeline.pdf>.

2. "Alexandre Edmond Becquerel." Molecular Expressions: Science, Optics and You - Timeline. N.p., n.d. Web. 1 Nov. 2013. <http://micro.magnet.fsu.edu/optics/timeline/people/becquerel.html>.

3. "Photovoltaic Technology Basics." Office of Energy Efficiency and Renewable Energy. N.p., n.d. Web. 18 Nov. 2013. <http://www.eere.energy.gov/basics/renewable_energy/types_silicon.html>.

4. Swiss Federal Laboratories for Materials Science and Technology (EMPA). "Understanding what makes a Thin Film solar cell efficient."ScienceDaily, 5 Nov. 2013. Web. 18 Nov. 2013.

5. Green, Martin (2003). *Third Generation Photovoltaics: Advanced Solar Energy Conversion*. Springer Science+Business Media.

6. "2012 Renewable Energy Data Book." *Energy Efficiency and Renewable Energy*. US Department of Energy, n.d. Web. 1 Nov. 2013. <http://www.nrel.gov/docs/fy14osti/60197.pdf>.

7. Yang F. et al. (2005). "Controlled growth of a molecular bulk heterojunction photovoltaic cell". *Nature Materials* **4**: 37–41.

8. Cowan, S. R.; Banerji, N.; Leong, W. L.; Heeger, A. J. *Adv. Funct. Mater.* **2012**, *22*, 1116-1128.

9. Chen, M.-H.; Hou, J.; Hong, Z.; Yang, G.; Sista, S.; Chen, L.-M.; Yang, Y. *Adv. Mater.* **2009**, *21*, 4238-4242.

10. Chen, H.-Y.; Hou, J.; Zhang, S.; Liang, Y.; Yang, G.; Yang, Y.; Yu, L.; Wu, Y.; Li, G. *Nature Photonics* **2009**, *3*, 649-653.

11. Zhang, Y.; Hau, S. K.; Yip, Y.-L.; Sun, Y.; Acton, O.; Jen, A. K.-Y. *Chem. Mater.* **2010**, *22*, 2696-2698.

12. Wienk, M. M.; Turbiez, M.; Gilot, J.; Janssen, R. A. J. *Adv. Mater.* **2008**, *20*, 2556-2560.

13. Park, S.; Roy, A.; Beaupre, S.; Cho, S.; Coates, N.; Moon, J. S.; Moses, D.; Leclerc, M.; Lee, K.; Heeger, A. J. *Nature Photonics* **2009**, *3*, 297-303.

14. Kruger, J.; Plass, R.; Cevey, L.; Piccirelli, M.; Gratzel, M. *Appl. Phys. Lett.* **2001**, *79*, 2085-2087.

15. Snaith, H. J.; Gratzel, M. *Appl. Phys. Lett.* **2006**, *89*, 262114(262113).

16. Snaith, H. J.; Moule, A. J.; Klein, C.; Meerholz, K.; Friend, R. H.; Gratzel, M. *Nano Lett.* **2007**, *7*, 3372-3376.

17. Liu, X.; Jeong, K.S.; Williams, B.P.; Vakhshouri, K.; Kondo, M.; Han, K.; Gomez, E.D.; Wang, Q., *Journal of Physical Chemistry B*, **2013**.

18. Wibowo, R.; Aldous, L.; Ward Jones, S.; Compton, R. G. *ECS Trans.* **2010**, *33*, 523-535.

19. Belhocine, T.; Forsyth, S. A.; Nimal Gunaratne, H. Q.; Nieuwenhuyzen, M.; Puga, A. V.; Seddon, K. R.; Srinivasan, G.; Whiston, K. *Green Chem.* **2011**, *13*, 59-63.

20. Snaith, H. J.; Schmidt-Mende, L.; Gratzel, M. *Phys. Rev. B* **2006**, *74*, 045306(045306).

ACADEMIC VITA

Bryan P. Williams
257 Yoder Road, Harleysville, PA 19438
Bpw5043@gmail.com

Education

The Pennsylvania State University – Schreyer Honors College
Bachelor of Science in Chemical Engineering – General Option Graduated: December 2013

Honors and Awards

Penn State University - Dean's List (All Semesters)
OXE Chemical Engineering National Honors Society
Virginia S. and Philip L. Walker Jr. Enrichment Scholarship
Lee and Mary Eagleton Award for Excellence in Design
Encore Award - Johnson & Johnson Consumer Inc.

Association Memberships/Activities

Atlas Benefitting THON – 2012 Finance & Administration Chair
American Institute of Chemical Engineers – 2013 Seminar Chair

Professional Experience

Quality EID Intern Avon, MA
General Electric Oil & Gas – Masoneilan Control Valves May 2013 – August 2013

External Manufacturing Operations Co-Op Skillman, NJ
Johnson & Johnson Consumer Companies, Inc June 2012- January 2013

Undergraduate Research Assistant & REU Participant University Park, PA
Department of Chemical Engineering, Gomez Polymer Electronics Lab 2010-2013

Professional Presentations

1st Place, Penn State AIChE Paper Presentation Competition – Spring 2013

Publications and Papers

Tuning the Dielectric Properties of Organic Semiconductors Via Salt Doping" Liu, X.; Jeong, K.S.; Williams, B.P.; Vakhshouri, K.; Kondo, M.; Han, K.; Gomez, E.D.; Wang, Q., Journal of Physical Chemistry B, 2013.